DOI: 10.22226/2410-3535-2019-1-86-90 PACS: 81.20.-n, 78.20.-e

Synthesis, structure and properties of $K_{2(1-x)}Rb_{2x}Al_2B_2O_7$ and $Cs_{1.39}Tl_{0.61}Al_2B_2O_7$ borates as the basis for preparing new oxide materials

V. G. Grossman[†,1], B. G. Bazarov[1], S. Y. Stefanovich[2], M. S. Molokeev[3,4], J. G. Bazarova[1]

[†]grossmanv@mail.ru

[1]Baikal Institute of Nature Management, Siberian Branch, RAS, 6 Sakhyanova St., Ulan-Ude, 670047, Russia
[2]Lomonosov Moscow State University, GSP-1, 1/3 Leninskie Gory, Moscow, 119991, Russia
[3]Kirensky Institute of Physics, Federal Research Center KSC, Siberian Branch, RAS, 50/38 Akademgorodok, Krasnoyarsk, 660036, Russia
[4]Siberian Federal University, 82 Svobodniy Av., Krasnoyarsk, 660041, Russia

With the development of technology, the need for highly efficient functional materials is steadily increasing. Currently, borates attract the attention of researchers, as they are promising nonlinear materials. Potassium rubidium aluminum borate based on potassium aluminum borate (trigonal syngony, space group $P321$, $Z=3$) was obtained by solid-phase synthesis. The individuality and purity of the borates were confirmed by X-ray diffraction. Analysis of differential scanning calorimetry and thermogravimetric method for $K_{2(1-x)}Rb_{2x}Al_2B_2O_7$ ($x=0.1-0.8$) was performed in the temperature range of 25–1075°C. Potassium rubidium borates decompose in the temperature range of 900–1000°C. Differential scanning calorimetry, dielectric loss tangent, and second-harmonic generation data revealed phase transitions for $K_{0.6}Rb_{1.4}Al_2B_2O_7$. A significant SHG effect was found at room temperature for $K_{0.6}Rb_{1.4}Al_2B_2O_7$ ($Q=70$). Then the SHG effect increases to $Q=85$ at a temperature of 645°C and remains constant with a further increase in temperature. The new triple borate $Cs_{1.39}Tl_{0.61}Al_2B_2O_7$ was synthesized by the solid-phase synthesis, and its crystallographic parameters were obtained by the Rietveld method. This borate crystallizes in the monoclinic space group $P2_{1/c}$ with the unit cell parameters: $Z=2$, $a=6.6669(3)$ Å, $b=7.2991(3)$ Å, $c=9.3589(4)$ Å, $\beta=116.6795(18)°$, $V=406.94(3)$ Å^3. The structure can be considered to be built up from the nearly planar $[Al_2B_2O_{10}]$ rings, which are composed of two AlO_4 tetrahedra and two BO_3 triangles, connected, alternately to each other by corner-sharing.

Keywords: borate, solid-phase synthesis, optical properties.

УДК: 661.653

Синтез, структура и свойства боратов $K_{2(1-x)}Rb_{2x}Al_2B_2O_7$ и $Cs_{1.39}Tl_{0.61}Al_2B_2O_7$ как основа получения новых оксидных материалов

Гроссман В. Г.[†,1], Базаров Б. Г.[1], Стефанович С. Ю.[2], Молокеев М. С.[3,4], Базарова Ж. Г.[1]

[†]grossmanv@mail.ru

[1]Байкальский институт природопользования СО РАН, ул. Сахьяновой, 6, Улан-Удэ, 670047, Россия
[2]Московский государственный университет им. М. В. Ломоносова, ГСП-1, Ленинские горы, 1/3, Москва, 119991, Россия
[3]Институт физики им. Л. В. Киренского ФИЦ КНЦ СО РАН, 50/38Академгородок, Красноярск, 660036, Россия
[4]Сибирский Федеральный Университет, Свободный пр., 79, Красноярск, 660041, Россия

С развитием технологии потребность в высокоэффективных функциональных материалах растет. В настоящее время бораты привлекают внимание исследователей, поскольку они являются перспективными нелинейными материалами. Твердофазным синтезом получены бораты $K_{2(1-x)}Rb_{2x}Al_2B_2O_7$ ($x=0.1-0.8$) на основе калий-алюминиевого бората (тригональная сингония, пространственная группа $P321$, $Z=3$). Индивидуальность и чистота боратов подтверждена рентгеновской дифракцией. Анализ дифференциально-сканирующей калориметрией и термогравиме-

трическим методом для $K_{2(1-x)}Rb_{2x}Al_2B_2O_7$ ($x = 0.1–0.8$) был проведен в интервале температур 25–1075°C. Калий-рубидиевые бораты разлагаются в интервале температур 900–1000°C. Дифференциальной сканирующей калориметрией, диэлектрическими измерениями и методом генерации второй оптической гармоники выявлены фазовые переходы для $K_{0.6}Rb_{1.4}Al_2B_2O_7$. Значительный ГВГ-эффект был обнаружен при комнатной температуре для $K_{0.6}Rb_{1.4}Al_2B_2O_7$ ($Q = 70$). Эффект генерации второй гармоники возрастает до $Q = 85$ при температуре 645°C и остается постоянным при дальнейшем увеличении температуры. Новый тройной борат $Cs_{1.39}Tl_{0.61}Al_2B_2O_7$ был синтезирован методом твердофазного синтеза, а его кристаллографические параметры были получены с помощью метода Ритвельда. Этот борат кристаллизуется в моноклинной пространственной группе $P2_{1/c}$ с параметрами элементарной ячейки: $Z = 2$, $a = 6.6669(3)$ Å, $b = 7.2991(3)$ Å, $c = 9.3589(4)$ Å, $\beta = 116.6795(18)°$, $V = 406.94(3)$ Å^3. Структуру можно представить в виде почти плоских колец $[Al_2B_2O_{10}]$, которые состоят из двух тетраэдров AlO_4 и двух BO_3 треугольников, соединенных попеременно друг с другом посредством вершин.

Ключевые слова: борат, твердофазный синтез, оптические свойства.

1. Introduction

Borates have attracted considerable attention because they have important practical applications as materials for nonlinear optical (NLO) effects, in particular optical second harmonic generation (SHG) and linear electro-optics effects (EOE) [1, 2]. For example, β-BaB_2O_4, LiB_3O_5, CsB_3O_5 and $YCa_4(BO_3)_3O$ are all well-known NLO materials [3]. In 1998, $K_2Al_2B_2O_7$ (KABO) as a new nonlinear optical crystal was reported by Hu et al. [4, 5]. The material crystallizes in space group $P321$ ($Z = 3$) with the unit cell parameters $a = b = 8.55800(2)$ Å, $c = 8.45576(3)$ Å [6]. In the structure of KABO, the nearly planar $(Al_3B_3O_6)$ networks perpendicular to the c-axis are connected to one another by bridging oxygen atoms, and the alkaline cations (K^+) are located between the layers. In the $(Al_3B_3O_6)$ unit, each Al^{3+} cation is linked with three terminal O atoms of the triangle $(BO_3)^{3-}$ groups and a bridging oxygen ion to form a tetrahedral $(AlO_4)^{5-}$ group.

Compared to β-BaB_2O_4 and $CsLiB_6O_{10}$, the KABO crystal is free of moisture and possesses smaller walk-off and larger acceptance angles than BBO crystals, stable chemical and physical properties, and good mechanical properties. All of these merits indicate that KABO may be a competitive candidate for the fourth harmonic generation of Nd^{3+} doped lasers, such as Nd:YAG, Nd:YLF and Nd:YVO_4, etc. However, the KABO crystal has a problem concerning abnormal absorptions in the 200–300 nm regions that greatly reduces the conversion efficiency of the fourth harmonic generation of Nd-based laser [7].

In order to improve the properties of KABO crystals, the structure and properties of doped KABO crystals were studied. The structure of Na-doped KABO was studied by Meng et al. [8–11], the growth and properties of Fe-doped KABO crystals were studied by Wang et al. [12,13]. $K_2(Al_{0.71}Ga_{0.29})_2B_2O_7$ (KAGBO) has a slightly smaller SHG coefficient and larger refractive indices [14].

Recently, a solid solution $K_{2(1-x)}Rb_{2x}Al_2B_2O_7$ with as high upper limit at room temperature as $x \sim 0.8$ has been discovered [15]. The vibrational properties and the electronic structure of borate $KRbAl_2B_2O_7$ (KRABO) are investigated in [16]. In [17], the ultraviolet nonlinear optical crystal (NLO) $K_{0.67}Rb_{1.33}Al_2B_2O_7$ (KRABO) was first obtained by the seed growth method. In this article, we continue to study the properties of $KRbAl_2B_2O_7$. Also in the present work, a new borate $Cs_{1.39}Tl_{0.61}Al_2B_2O_7$, isostructural to $Cs_2Al_2B_2O_7$ [18] has been obtained.

2. Experimental

Polycrystalline samples of $K_{2(1-x)}Rb_{2x}Al_2B_2O_7$ ($x = 0.1$, 0.2, 0.3, 0.4, 0.5, 0.6, 0.7 and 0.8) and $CsTlAl_2B_2O_7$ were prepared by solid-state synthesis using a mixture of $Al(NO_3)_3 \cdot 9H_2O$ (pure), H_3BO_3 (chemically pure grade), K_2CO_3 (chemically pure grade), Rb_2CO_3 (chemically pure grade), $CsNO_3$ (pure for analysis), $TlNO_3$ (pure for analysis) in stoichiometric ratio as starting materials. Initially, to minimize the content of water captured from the environment, the carbonates and nitrates were annealed at 300°C in dry air flow. The mixture of $K_{2(1-x)}Rb_{2x}Al_2B_2O_7$ ($x = 0.1$, 0.2, 0.3, 0.4, 0.5, 0.6, 0.7 and 0.8) was ground in an agate mortar and first heated at 300°C, then slowly heated to 800°C for several days [15]. $CsTlAl_2B_2O_7$ was synthesized according to the following annealing scheme. The charges were first fired at 120°C for 1 hour, at 150°C for 1 hour, at 220°C for 3 hours, at 300°C for 5 hours, at 350°C for 15 hours, then chaffed and heated the next time at 400°C for 7 hours, at 450°C for 40 hours, at 520°C for 40 hours, at 600°C for 48 hours, at 700°C for 20 hours, at 800°C for 45 hours, and at 850°C for 25 hours. Repeated grindings are performed between sintering processes to improve the homogeneity of mixing. All products are obtained after natural cooling to room temperature. X-ray powder diffraction was used to identify the product.

The powder X-ray diffraction was recorded on a Bruker D8 ADVANCE X-ray diffractometer (Bruker, Berlin, Germany) with Cu-K_α radiation ($\lambda = 1.5418$ Å) at room temperature. The scanning range is between 8 and 100° with a scanning width of 0.02 and a rate of 0.1° s^{-1}.

The thermal property was investigated by the differential scanning calorimetric (DSC) analysis and the thermogravimetric analysis (TGA) using a NETZSCH STA 449C TG/DSC/DTA thermal analyzer (NETZSCH, Berlin, Germany). A 15 mg sample of powder was placed in a Pt crucible and heated from room temperature at a rate of 10°C · min^{-1} in an Ar atmosphere.

The measurement of second harmonic generation (SHG) was carried out on polycrystalline samples. The minilite-I Nd: YAG laser operating in Q-switched mode at a repetition rate of 10 Hz produced the frequency doubling from $\lambda_\omega = 1064$ nm to the second harmonics, $\lambda_{2\omega} = 532$ nm in the sample. The green light of the second harmonics was collected with the lens and then directed to the photomultiplier tube. To detect the light only at 532 nm, a narrow band-pass interference filter was attached to the photomultiplier. The measured

signal intensity ($I_{2\omega}$) from the sample was calibrated in relation to the α-quartz powder standard with a grain size of 3 μm. $Q = I_{2\omega}/I_{2\omega}(SiO_2)$ quantitatively presents the SHG activity of the sample.

The dielectric loss tangent (tgα) was measured on a Novocontrol Beta-N impedance-analyzer in a ProboStat measuring cell using the double-contact method [19] in the frequency range of 0.3 Hz–1 MHz on heating at 20–850°C with 2°C·min^{-1}; ceramic pellets were 10 mm in diameter and 2 mm in height.

3. Results and discussion

Thermogravimetric (TG) and differential thermal analyses (DTA) were performed on $K_{2(1-x)}Rb_{2x}Al_2B_2O_7$ ($x = 0.1–0.8$) samples. The results are presented for $KRbAl_2B_2O_7$ in Fig. 1. The temperature of the phase transition for $KRbAl_2B_2O_7$ corresponds to 714°C, $\Delta H = -1.321$ J/g.

For all samples, a mass loss and one endothermic effect, which corresponds to the temperature of the phase transition, was observed in the temperature range of 900–1000°C (Fig. 1, 2). The mass loss of the sample is due to the decomposition of $K_{2(1-x)}Rb_{2x}Al_2B_2O_7$ ($x = 0.1–0.8$).

The dependence of the temperature of phase transitions of solid solutions $K_{2(1-x)}Rb_{2x}Al_2B_2O_7$ on the parameter x is shown in Fig. 2.

An increase in the content of rubidium leads to a decrease in the temperature of the phase transition. It is known that there was a KABO-type structure detected for a powder sample with a nominal composition $x = 0.9$ and the solubility limit in $K_{2(1-x)}Rb_{2x}Al_2B_2O_7$ crystals can be estimated as $x \sim 0.83–0.9$ at ambient conditions. In this connection, the temperature of the phase transition only for the composition $x = 0.8$ was determined.

A decrease in the temperature of the phase transition agrees with the fact that an increase in the rubidium content results in a quasilinear increase of the unit cell parameters and the cell volume [15].

A significant effect of SHG was found at room temperature for $K_{0.6}Rb_{1.4}Al_2B_2O_7$ $Q = 70$ (Fig. 3). The signals confirm the absence of an inversion center. Then the effect of SHG increases to 85 at a temperature of 645°C and remains constant with a further increase in temperature. When cooled, the effect of SHG slightly decreases, but it does not drop below $I_{2\omega}/I_{2\omega}(SiO_2) = 65$.

Fig. 4 shows the temperature dependences of the dielectric loss tangent for $K_{0.6}Rb_{1.4}Al_2B_2O_7$. The maxima of dielectric losses characteristic of the relaxational type, which with increasing frequency shift to higher temperatures, are revealed. Anomalies in dielectric loss tangent were revealed in the vicinity of 645°C, independent of the measurement frequency.

The diffraction data for the Rietveld analysis were collected at room temperature (27°C) with a Bruker D8 ADVANCE powder diffractometer in the Bragg-Brentano geometry and a Vantec linear detector. The operating parameters were:

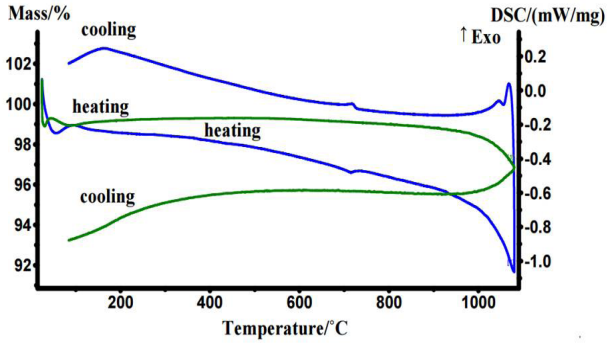

Fig. 1. DSC and TG curves of $KRbAl_2B_2O_7$.

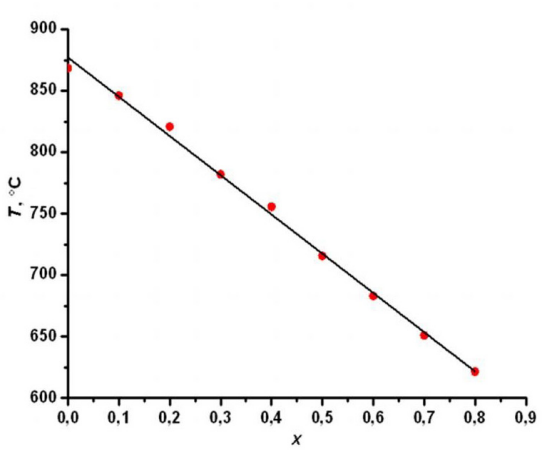

Fig. 2. Dependences of the temperature of phase transitions on composition in solid solutions $K_{2(1-x)}Rb_{2x}Al_2B_2O_7$ ($x = 0.1–0.8$).

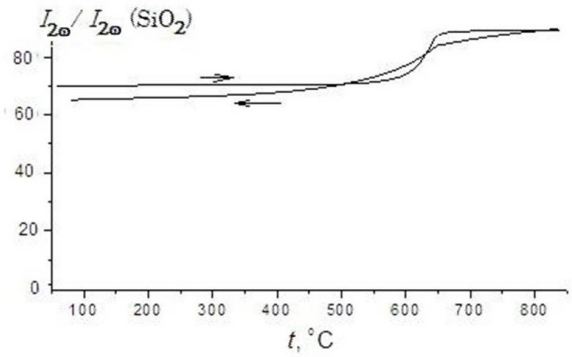

Fig. 3. Heating temperature dependence of SHG signals for $K_{0.6}Rb_{1.4}Al_2B_2O_7$.

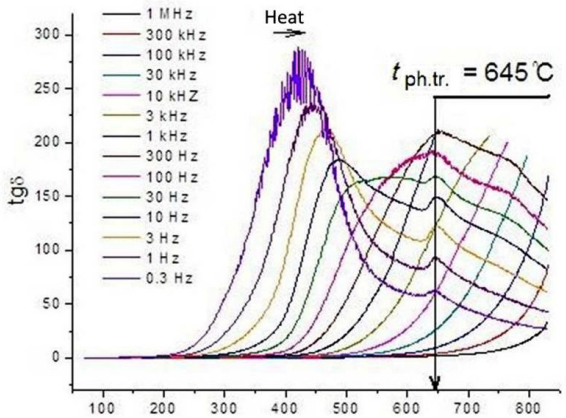

Fig. 4. (Color online) Dependence of dielectric loss tangent (tgδ) $K_{0.6}Rb_{1.4}Al_2B_2O_7$ on temperature.

Cu-K_α radiation, step size 0.02°. Data were collected in the range of 2θ from 8 to 100°. Peak positions were determined with the EVA program, available in the PC DIFFRAC-PLUS software package supplied by Bruker. X-ray patterns of the title compound were indexed using the ITO program [20]. Replacement of cesium atoms by thallium ones in the compound $Cs_2Al_2B_2O_7$ facilitates the formation of the phase $Cs_{1.39}Tl_{0.61}Al_2B_2O_7$. For the finer structure analysis of $Cs_{1.39}Tl_{0.61}Al_2B_2O_7$ the single crystal data on the phase $Cs_2Al_2B_2O_7$, which crystallizes in the space group $P2_{1/c}$, were used [18]. The refinement of atomic positions and occupancy of atoms leads to the formula: $Cs_{1.39}Tl_{0.61}Al_2B_2O_7$.

The experimental and theoretical X-ray diffraction patterns obtained for $Cs_{1.39}Tl_{0.61}Al_2B_2O_7$ are shown in Fig. 5.

A good relation between experimental and theoretical curves is evident.

The parameters of the refinement and atomic coordinates of $Cs_{1.39}Tl_{0.61}Al_2B_2O_7$ are shown in Tables 1 and 2, respectively. The main lengths of interatomic bonds are given in Table S1 (Supplementary Material).

The structure of $Cs_{1.39}Tl_{0.61}Al_2B_2O_7$ is shown in Fig. 6.

This is a three-dimensional framework built from corner-sharing AlO_4 tetrahedra and BO_3 triangles with channels occupied by the Cs^+ and Tl^+ cations. The structure can be considered to be built up from the nearly planar $[Al_2B_2O_{10}]$ rings, which are composed of two AlO_4 tetrahedra and two BO_3 triangles, connected alternately to each other by corner-sharing.

$Rb_2Al_2B_2O_7$, $Cs_2Al_2B_2O_7$, $Cs_{1.39}Tl_{0.61}Al_2B_2O_7$ crystallize in the space group $P2_{1/c}$. The structure of these borates consists of AlO_4 tetrahedra and BO_3 triangles. The unit cell of $Rb_2Al_2B_2O_7$ (a = 8.901(2) Å, b = 7.539(1) Å, c = 11.905(2) Å, β = 103.97(1)°, V = 775.3(2) Å^3) is almost twice as large as that of $Cs_2Al_2B_2O_7$ (a = 6.719(1) Å, b = 7.121(1) Å, c = 9.626(3) Å, β = 115.3(1)°, V = 416.5(2) Å^3) and $Cs_{1.39}Tl_{0.61}Al_2B_2O_7$ (a = 6.6669(3) Å, b = 7.2991(3) Å, c = 9.3589(4) Å, β = 116.6795(18)°, V = 406.94(3) Å^3). $Rb_2Al_2B_2O_7$ differs from $Cs_2Al_2B_2O_7$ and $Cs_{1.39}Tl_{0.61}Al_2B_2O_7$ in that the bond angle of the bridging Al-O-Al, equal to 146.9(2)°, is less than the bond angle in borates $Cs_2Al_2B_2O_7$ and $Cs_{1.39}Tl_{0.61}Al_2B_2O_7$ (the bond angle is 180°).

The bond distances and bond angles in $Cs_{1.39}Tl_{0.61}Al_2B_2O_7$ are well compared with the related structures $M_2Al_2B_2O_7$ (M = Na, K, Rb) [6,21,22]. AlO_4 is a slightly distorted tetrahedron with the Al-O bond distances ranging from 1.637(18) Å to 1.77(2) Å. In the BO_3 triangles, the lengths of the B-O bonds range from 1.27(3) to 1.41(3) Å. The distances of Cs-O in $Cs_{1.39}Tl_{0.61}Al_2B_2O_7$ range from 2.967(13) to 3.4160(16) Å, which resemble those in $Cs_2Al_2B_2O_7$ [18] (3.070(3) to 3.600(3) Å).

The DSC (Differential Scanning Calorimetry) curve exhibits one endothermic peak on the heating curve at 900°C, accompanied by the apparent weight loss observed on the TG (Thermogravimetric Analysis) curve (Fig. 7). The XRD pattern indicates that the molten residues were mainly raw materials instead of the original compound, which clearly demonstrates that 900°C is the decomposition temperature. Hence, $Cs_{1.39}Tl_{0.61}Al_2B_2O_7$ melts incongruently.

Table 1. Crystallographic parameters of $Cs_{1.39}Tl_{0.61}Al_2B_2O_7$.

Space group	$P2_{1/c}$
a, Å	6.6669(3)
b, Å	7.2991(3)
c, Å	9.3589(4)
β, °	116.6795(18)
V, Å^3	406.94(3)
Z	2
2θ-interval range, °	8 –100
R_p, %	3.994
R_{wp}, %	5.115
R_{exp}, %	3.248
R_{Bragg},%	1.33
χ^2	2.481

Table 2. Atomic coordinates and isotropic thermal parameters (B_{iso}) in the structure of $Cs_{1.39}Tl_{0.61}Al_2B_2O_7$ at room temperature.

Atom	x	y	z	B_{iso}*/B_{eq}
Cs	0.7831(3)	0.3661(3)	0.10928(19)	3.2(2)
Tl	0.7831(3)	0.3661(3)	0.10928(19)	3.2(2)
Al	0.2418(12)	0.1147(16)	0.0416(9)	2.2(3)
B	0.372(5)	0.393(5)	0.274(4)	2
O1	0.258(3)	0.336(2)	0.125(2)	2
O2	0.254(3)	0.346(2)	0.3614(19)	2
O3	0	0	0	2
O4	0.546(3)	0.4949(19)	0.331(2)	2

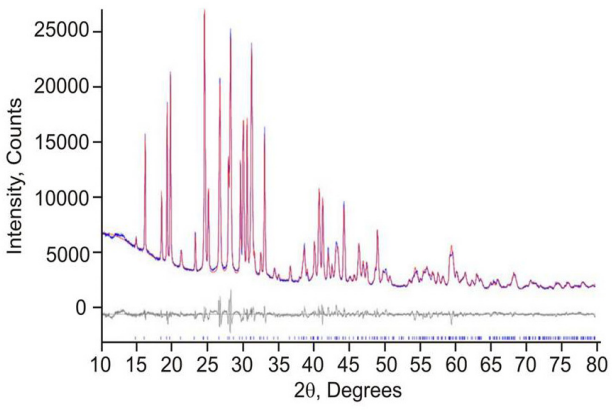

Fig. 5. X-ray diffraction patterns recorded and calculated for $Cs_{1.39}Tl_{0.61}Al_2B_2O_7$ at room temperature.

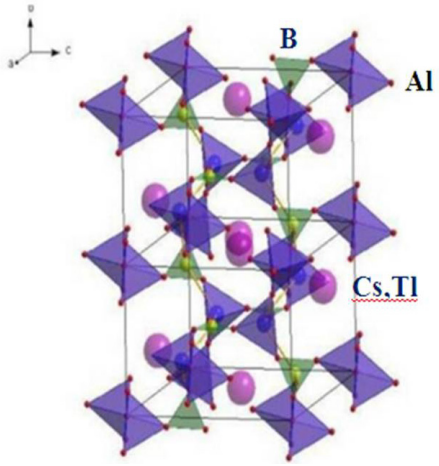

Fig. 6. (Color online) The crystal structure of $Cs_{1.39}Tl_{0.61}Al_2B_2O_7$ at room temperature.

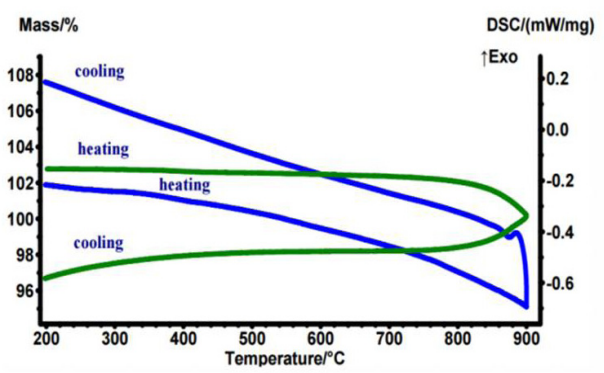

Fig. 7. DSC and TG curves of $Cs_{1.39}Tl_{0.61}Al_2B_2O_7$.

4. Conclusions

The $K_{2(1-x)}Rb_{2x}Al_2B_2O_7$ crystals possess nonlinear optical properties and can be used for frequency conversion. Isovalent substitution of Rb^+ ions for K^+ ions in the KABO lattice results in a decrease in the phase transition temperature from 869°C for $K_2Al_2B_2O_7$ to 621°C for $K_{0.4}Rb_{1.6}Al_2B_2O_7$. A comprehensive study of DSC, SHG, and dielectric loss tangent made it possible to reveal anomalies associated with structural phase transitions. A new borate $Cs_{1.39}Tl_{0.61}Al_2B_2O_7$ was synthesized and its structure in space group $P2_{1/c}$ was determined through Rietveld X-ray powder diffraction analysis.

Acknowledgement. The research was carried out within the state assignment of FASO of Russia (Theme No 0339-2016-0007).

Supplementary Material. *The online version of this paper contains supplementary material (table) available free of charge at the journal's Web site (lettersonmaterials.com).*

References

1. C. Chen, Z. Lin, Z. Wang. Applied Physics. 80, 1 (2005). DOI: 10.1007/s00340-004-1645-9

2. Z.-G. Hu, M. Yoshimura, Y. Mori, T. Sasaki. J. Crystal Growth. 275 (1), 232 (2005). DOI: 10.1016/j.jcrysgro.2004.10.160

3. P. Becker. Advanced Materials. 10 (13), 979 (1998). DOI: 10.1002/(SICI)1521-4095(199809)10:13<979::AID-ADMA979>3.0.CO;2-N

4. Z.G. Hu, Y. Mori, T. Higashiyama, Y.K. Yap, Y. Kagebayash, T. Sasaki. Proceedings of SPIE. 3556, 156 (1998). DOI: 10.1117/12.318262

5. N. Ye, W. Zeng, J. Jiang, B. Wu, C. Chen, B. Feng, X. Zhang. Journal of the Optical Society of America B. 17 (5), 764 (2000). DOI: 10.1364/JOSAB.17.000764

6. Z.G. Hu, T. Higashiyama, M. Yoshimura, Y. Mori, T.Z. Sasaki. Zeitschrift für Kristallographie — New Crystal Structures. 214 (4), 433 (1999).

7. L.J. Liu, C.L. Liu, X.Y. Wang, Z.G. Hu, R.K. Li, C.T. Chen. Solid State Sciences. 11 (4), 841 (2009). DOI: 10.1016/j.solidstatesciences.2009.01.003

8. X.Y. Meng, J.H. Gao, Z.Z. Wang, R.K. Li, C.T. Chen. Journal of Physics and Chemistry of Solids. 66 (10), 1655 (2005). DOI: 10.1016/j.jpcs.2005.06.002

9. W. Zhenxiong, Y. Yinchao, W. Lirong, W. Guiling, H. Zhanggui. Optical Materials. 34 (9), 1575 (2012). DOI: 10.1016/j.optmat.2012.03.023

10. M. He, X.L. Chen, H. Okudera, A. Simon. Chemistry of Materials. 17 (8), 2193 (2005). DOI: 10.1021/cm050142y

11. Y.C. Yue, Z.X. Wu, Z.S. Lin, Z.G. Hu. Solid State Sciences. 13 (5), 1172 (2011). DOI: 10.1016/j.solidstatesciences.2010.11.028

12. Y.G. Wang, R.K. Li. Optical Materials. 32 (10), 1313 (2010). DOI: 10.1016/j.optmat.2010.04.036

13. Y.G. Wang, R.K. Li. Journal of Solid State Chemistry. 183 (6), 1221 (2010). DOI: 10.1016/j.jssc.2010.03.037

14. X Wang, R.K. Li. Optical Materials. 45, 197 (2015). DOI: 10.1016/j.optmat.2015.03.037

15. V.V. Atuchin, B.G. Bazarov, T.A. Gavrilova, V.G. Grossman, M.S. Molokeev, Z.G. Bazarova. Journal of Alloys and Compounds. 515, 119 (2012). DOI: 10.1016/j.jallcom.2011.11.115

16. V.V. Atuchin, S.V. Adichtchev, B.G. Bazarov, Zh.G. Bazarova, T.A. Gavrilova, V.G. Grossman, V.G. Kesler, G.S. Meng, Z.S. Lin, N.V. Surovtsev. Materials Research Bulletin. 48, 929 (2013). DOI: 10.1016/j.materresbull.2012.10.055

17. Q. Huang, L. Liu, M. Xia, Y. Yang, S. Guo, X. Wang, Z. Lin, C. Chen. Crystals. 7, 2 (2017). DOI: 10.3390/cryst7040104

18. F. Kai, Yin Wenlong, Y. Jiyong, W.J. Yicheng. Journal of Solid State Chemistry. 184 (12), 3353 (2011). DOI: 10.1016/j.jssc.2011.10.023

19. R.W. Vest, N.M. Tallan. Journal of Applied Physics. 36, 543 (1965).

20. J.W. Visser. Journal of Applied Crystallography. 2, 89 (1969).

21. M. He, X.L. Chen, T. Zhou, B.Q. Hu, Y.P. Xu, T.Xu. Journal of Alloys and Compounds. 327 (1), 210 (2001). DOI: 10.1016/S0925-8388(01)01561-4

22. J.L. Kissick, D.A. Keszler. Acta Crystallographica Section E. 58 (10), 185 (2002). DOI: 10.1107/S1600536802015659